

”Leading blob” model in a stochastic acceleration scenario: the case of the 2009 flare of Mkn 501

E. Lefa^{1,2}

¹ Max-Planck-Institut für Kernphysik, P.O. Box 103980, 69029 Heidelberg, Germany

² Landessternwarte, Königstuhl 12, 69117 Heidelberg, Germany

eva.lefa@mpi-hd.mpg.de

F.A. Aharonian^{1,3}

¹ Max-Planck-Institut für Kernphysik, P.O. Box 103980, 69029 Heidelberg, Germany

³ Dublin Institute for Advanced Studies, 31 Fitzwilliam Place, Dublin 2, Ireland

and

F.M. Rieger^{1,4}

¹ Max-Planck-Institut für Kernphysik, P.O. Box 103980, 69029 Heidelberg, Germany

⁴ European Associated Laboratory for Gamma-Ray Astronomy, jointly supported by
CNRS and MPG

Received _____; accepted _____

ApJ, to be submitted

ABSTRACT

Evidence for very hard, intrinsic γ -ray source spectra, as inferred after correction for absorption in the extragalactic background light (EBL), has interesting implications for the acceleration and radiation mechanisms acting in blazars. A key issue so far has been the dependance of the hardness of the γ -ray spectrum on different existing EBL models. The recent *Fermi* observations of Mkn 501 now provide additional evidence for the presence of hard intrinsic γ -ray spectra independent of EBL uncertainties. Relativistic Maxwellian-type electron energy distributions that are formed in stochastic acceleration scenarios offer a plausible interpretation for such hard source spectra. Here we show that the combined emission from different components with Maxwellian-type distributions could in principle also account for more softer and broader, power law-like emission spectra. We introduce a "leading blob" scenario, applicable to active flaring episodes, when one (or few) of these components become distinct over the "background" emission, producing hard spectral features and/or hardening of the observed spectra. We show that this model can explain the peculiar high-energy characteristics of Mkn 501 in 2009, with evidence for flaring activity and strong spectral hardening at the highest γ -ray energies.

Subject headings: BL Lacertae objects: general - BL Lacertae objects: individual (Mkn 501) – diffuse radiation – galaxies: active - radiation mechanisms: non thermal

1. Introduction

Blazars are prominent γ -ray emitters with many peculiar features, the origin of which are currently discussed intensively in the general context of their multi-wavelength properties. During the last years two distinct features have attracted special attention: variability detected at very short timescales and the origin of very hard, intrinsic γ -ray source spectra when absorption in the Extragalactic Background Light (EBL) is taken into account. Although the observed TeV spectra of these sources are steep, their de-absorbed (EBL-corrected) spectra appear intrinsically hard. Current uncertainties on the EBL flux level and spectrum (cf. Primack et al. 2011 for a recent review) introduce difficulties in defining how hard the absorption-corrected source spectra are. However, in some characteristic cases, like for the distant blazars 1ES 1101-232 ($z = 1.86$) and 1ES 0229+200 ($z = 0.139$), the emitted spectra still tends to be very hard, with an intrinsic photon index $\Gamma \leq 1.5$, even when corrected for low EBL flux levels (Aharonian et al. 2006, 2007).

The recent *Fermi* detection of variable γ -ray emission from the nearby ($z = 0.034$) TeV blazar Mkn 501 in 2009 now removes this point of uncertainty, providing strong evidence for hard intrinsic γ -ray source spectra independently of questions related to the EBL. As already indicated in the original *Fermi* paper on Mkn 501 (Abdo et al. 2011), the spectrum above 10 GeV seems to become much harder during a (~ 30 -day) flaring state. A recent, independent analysis of the same data by Neronov et al. (2011) shows that the (10 GeV-200 GeV) flare spectrum could be as hard as $\Gamma \simeq 1.1$. While the *Fermi* collaboration did not comment much on the possible origin of the hard flare spectrum, Neronov et al. (2011) put forward the hypothesis that the hard spectrum flare could result from an electromagnetic cascade in the intergalactic medium, provided that the strength of the intergalactic magnetic field is smaller than 10^{-16} G and that primary γ -rays with 100 TeV can escape from the central compact region.

The noted small photon indices are generally not easy to achieve in standard leptonic scenarios, i.e., synchrotron self-Compton (SSC) or external Compton (EC) models, because radiative cooling tends to produce particle energy distributions that are always steeper than $dN/dE \propto E^{-2}$, irrespective of the initially injected particle spectrum. The corresponding TeV photon index would then be $\Gamma \geq 1.5$. Moreover, as the emission from these objects peaks at very high energies where suppression of the cross-section due to Klein-Nishina effects becomes important, even steeper intrinsic photon spectra are to be expected.

Hence, at first glance, hard γ -ray spectra might be somewhat easier to achieve in hadronic scenarios like the proton synchrotron model. For a proton spectra of, e.g., $dN_p/dE = AE^{-s} \exp[-(E/E_0)^\beta]$ the γ -ray spectrum would be $E_\gamma dN_\gamma/dE_\gamma \propto \nu^{-(s-1)/2} \exp[-(\nu/\nu_0)^{\beta/\beta+2}]$. Thus at energies below the synchrotron cutoff $h\nu_c \leq 300\delta$ GeV (Aharonian 2000) very hard γ -ray spectra may occur. For the magnetic field $B \sim 100$ G required in such models, the protons responsible for γ -rays below $h\nu_c$ are not effectively cooled. Hence, for $s \leq 2$, the γ -ray spectrum could be harder than $\nu F_\nu \propto \nu^{1/2}$, with the hardest possible $\nu F_\nu \propto \nu^{4/3}$ in the case of pile-up type proton distributions that might be realized in, e.g., converter-type particle acceleration mechanisms (Derishev et al. 2003).

On the other hand, in the context of leptonic models we know that very narrow electron distributions are able to produce hard γ -ray source spectra. These can be either power-law distributions with large value of the minimum cut-off, provided the magnetic field is sufficiently small to avoid radiative losses (Katarzyński et al. 2007; Tavecchio et al. 2009), or provided adiabatic losses dominate (Lefa et al. 2011). Alternatively, relativistic Maxwell-like distributions formed by a stochastic acceleration process that is balanced by radiative losses can be a viable option (Lefa et al. 2011). In both cases VHE spectra as hard as $E_\gamma dN/dE_\gamma \propto E_\gamma^{1/3}$ for the SSC case, and $E_\gamma dN/dE_\gamma \propto E_\gamma$ for EC models can be generated. Maxwellian-type particle distributions are especially attractive for the

interpretation of the inferred hard γ -ray source spectra because they resemble to some extent mono-energetic distributions (the hardest possible injection spectra). An important question that arises however then is, whether such distributions can also account for more softer and broader photon spectra.

Interestingly, the hard high-energy component of Mkn 501 emerged in a flaring state in May 2009, during which little flaring activity was detected at energies below 10 GeV. This suggests that the flare is related to an emission zone that is confined both in space (compact) and time (short, on a timescale of ~ 30 days). Additionally, there is no evidence for a similar, simultaneous increase at X-ray energies (Abdo et al. 2011).

Here we propose a leptonic multi-zone scenario that can accommodate softer emission spectra as well as flaring episodes with hard spectral features, like the one observed in Mkn 501. In this scenario, the observed radiation comes from several emitting regions ("blobs"), in which electrons are accelerated to relativistic energies through stochastic acceleration, forming pile-up distributions. All blobs are considered to have similar parameters apart from the characteristic energies ("temperatures") of their Maxwell-like distributions. We note that a "multi-blob" scenario, with power-law components characterized by different trajectories (viewing angles) has also been proposed in the past to account for the TeV emission from non-aligned AGNs (Lenain et al. 2008). What distinguishes the model introduced here is that, due to acceleration and losses, each component is considered to only carry a narrow (pile-up) particle distribution, with broad spectra being formed by an ensemble of components. We show, for example, that in the case where the total energy of the particles is the same for all blobs, the combined emission leads to a spectrum very similar to the one arising from a power-law distribution $dN/dE \propto E^{-p}$ with index $p = 2$. On the other hand, distinct spectral feature can appear once a leading zone dominates. This could happen, for example, if (a) the value of the temperatures

changes from blob to blob, and/or if (b) the energetics of a single blob changes.

2. A multi-zone scenario

Let us consider N regions in which electrons are stochastically accelerated (e.g., by scattering off randomly moving Alfvén waves) up to energies where acceleration is balanced by synchrotron or inverse Compton (Thomson) losses. Their steady-state energy distributions $n(\gamma) \propto \gamma^2 f(\gamma)$ then take on a relativistic Maxwellian-type form (Schlickeiser 1985; Aharonian et al. 1986)

$$n_i(\gamma) = A_i \gamma^2 e^{-\left(\frac{\gamma}{\gamma_{c_i}}\right)^b}, \quad (1)$$

($b \neq 0$; $i = 1, \dots, N$) with exponential cut-off Lorentz factor

$$\gamma_{c_i} = \left(\frac{bD_0}{\beta_s}\right)^{1/b} (m_e c^2)^{-1}, \quad (2)$$

and normalization factor A_i . Here, β_s refers to energy losses due to synchrotron radiation given by

$$\frac{dp}{dt} = -\beta_s p^2 = -\frac{4}{3}(\sigma_T/m_e^2 c^2) U_B p^2, \quad (3)$$

and the constant D_0 is given by the diffusion coefficient $D_p = \frac{p^2}{3\tau} \left(\frac{V_A}{c}\right)^2 \equiv D_0 p^{1-b}$, with $V_A = \frac{B}{\sqrt{4\pi\rho}}$ the Alfvén speed and $\tau = \lambda/c \propto p^{b-1}$, $b \geq 1$, the mean scattering time (Lefa et al. 2011). The shape of the exponential cut-off (characterized by the parameter b) is related to the turbulence wave spectrum $W(k) \propto k^{-q}$ as $b = q$. Note that if the particle distributions would be shaped by inverse Compton cooling in the Klein-Nishina regime, a smoother exponential cut-off is expected (e.g., Stawarz & Petrosian 2008).

For simplicity, we consider below the situation where all blobs have similar properties (e.g., magnetic field strength, linear size, Doppler factor) but different values for the characteristic energy γ_{c_i} . In the case of synchrotron losses and scattering off Alfvén waves, γ_{c_i} depends on the magnetic field and the bulk density of the flow. Thus, the modification

in γ_{c_i} that we assume for each blob might be related to a non-homogeneous bulk flow. The total energy density E_i that the relativistic particles gain through scattering off Alfvén waves is calculated to be

$$E_i = \int_1^\infty \gamma n_i(\gamma) d\gamma m_e c^2 = A_i m_e c^2 \frac{\gamma_{c_i}^4}{b} \Gamma\left[\frac{4}{b}, \frac{1}{\gamma_{c_i}^b}\right], \quad (4)$$

where $\Gamma[a, z]$ is the incomplete Γ function. We can now express the normalization factor as a function of the "temperature" (γ_{c_i}) and the energy E_i ,

$$A_i = \frac{E_i b}{m_e c^2 \gamma_{c_i}^4 \Gamma\left[\frac{4}{b}, \frac{1}{\gamma_{c_i}^b}\right]}, \quad (5)$$

which decreases as the cut-off energy increases, with a dependency well approximated by $A_i \propto \gamma_c^{-4}$ for all values of the coefficient b of interest. This is easily seen if we change the lower limit of the previous integration to 0, in which case the result becomes

$$A_i = \frac{4E_i}{m_e c^2 \gamma_{c_i}^4 \Gamma[(4+b)/b]}, \quad (6)$$

with $\Gamma[z]$ denoting the Γ function.

The combination of the above electron distributions can lead to power-law-like particle distributions if the temperatures of the different components do not differ significantly and if the components contribute equally to the overall spectra. The power-law index then essentially depends on the amount of energy given to the non-thermal particles in each blob, i.e., on how the total energy E_i of each component scales with temperature (γ_{c_i}). Steep spectra may arise if, e.g., the low temperature components dominate whereas harder spectra may occur if more energy is contained in the high-temperature blobs.

In Fig. 1 an example for the total differential electron number is shown assuming $E_i = \text{constant}$. For the plot, an exponential cut-off index $b = 2$ and $N = 4$ have been chosen. The temperatures are equally spaced on logarithmic scale. Then, the total energy distribution approximately forms a power-law $dN_e/d\gamma \propto \gamma^{-s}$ with index $s \simeq 2$ between

the minimum and maximum temperatures. As discussed above, this "special" value of the power-law index results from the assumption that all blobs have the same total energy, so that $\gamma^2 dN_e/d\gamma$ is the same for each zone. This can be demonstrated more formally by looking for the "envelope", i.e., the mathematical function that describes the curve which is tangent to each of the curves n_i in the $(dN_e/d\gamma, \gamma_c)$ plane at some point. This function approximates the sum of the energy distribution of the different components as $N \gg 1$ and gives the characteristic behavior of the total distribution above the minimum and below the maximum temperature. It can be found by solving the set of equations

$$F(\gamma, \gamma_c) = 0, \quad \vartheta_{\gamma_c} F(\gamma, \gamma_c) = 0, \quad (7)$$

where $F(\gamma, \gamma_c) \equiv dN_e/d\gamma - A(\gamma_c) \gamma^2 \exp[-(\gamma/\gamma_c)^b]$. If we assume that the energy in non-thermal particles is the same for each component, then we find

$$dN_e/d\gamma = c'(b) \gamma^{-2}, \quad \gamma_{c,\min} < \gamma < \gamma_{c,\max}, \quad (8)$$

where $c'(b) = 4(4/b)^{4/b} e^{-b/4} / m_e c^2 \Gamma[\frac{4+b}{b}]$ (cf. Fig. 1). On the other hand, if particle acceleration to higher energies goes along with a decrease in total energy, e.g., $E \propto 1/\gamma_c$, then steeper power law spectra can appear, i.e., $\frac{dN_e}{d\gamma} \propto \gamma^{-3}$. Note that in all these cases, radiative cooling is already taken into account.

Note that changing the total energy with γ_{c_i} in each component could also be interpreted as changing the number of contributing blobs as a function of γ_{c_i} , assuming that each component has the same energy. This could be formally accommodated by introducing a statistical weight w_i , so that the overall spectrum is expressed as

$$dN_e/d\gamma = \sum_{i=1}^{i=N} w_i n_i(\gamma). \quad (9)$$

Harder spectra may then occur, for example, if more blobs with higher temperatures exist and vice versa. Hence, a conclusion similar to the above can be drawn, once the statistical

weights vary correspondingly with temperature (γ_{ci}). In a continuous analogue, we may write

$$dN_e/d\gamma = \sum_{i=1}^{i=N} w_i n_i(\gamma) \rightarrow \int_{T_1}^{T_N} W(T) n(\gamma, T) dT \quad (10)$$

where $W(T)$ is the spectrum of the number of components per temperature. Since Maxwellian-type electron distributions behave, to some extent, like mono-energetic ones, the total energy distribution between the minimum and the maximum temperature mimics the spectrum of the number of the blobs $W(T)$ (provided $W(T)$ does not rise quicker than T^2). Thus, in principle a variety of spectra may arise, depending on the choice of $W(T)$. Conversely, observations of extended power law-like energy distributions then impose constraints on how $W(T)$ of a source can vary with temperature.

The SSC spectrum, arising as the sum of the different Maxwell-like distributions of Fig. 1, is shown in Fig. 2. The synchrotron flux resembles the flux that would be emitted by a power-law particle distribution of index 2. Between the frequencies related to the minimum and maximum temperatures, $\nu_{\min} \propto B\gamma_{c,\min}^2$ and $\nu_{\max} \propto B\gamma_{c,\max}^2$ it exhibits a $F_\nu \propto \nu^{-1/2}$ behavior. For $\nu < \nu_{\min}$ it follows the characteristic $F_\nu \propto \nu^{1/3}$ synchrotron emissivity function, while for $\nu \geq \nu_{\max}$ the exponential cut-off becomes smoother $F_\nu \propto \exp[-(\nu/\nu_{\max})^{\frac{b}{2+b}}]$ (Fritz 1989; Zirakashvili & Aharonian 2007).

In the present model, the electrons in each blob are considered to only up-scatter their own synchrotron photons and not the ones emitted from the other blobs. The photon fields produced by the other components therefore do not contribute to the emitted Compton spectrum of each blob. In the Thomson regime then the up-scattered photon spectrum again approaches a power-law behavior similar to the synchrotron one, i.e. $F_\nu \propto \nu^{-1/2}$. Once Klein-Nishina effects become important, the suppression of the cross-section makes the high-energy spectrum steeper, as expected. In the case of discrete zones, where the particle distributions and synchrotron photons are almost mono-energetic, this happens

at (intrinsic) energies greater than $\gamma_{c_i}(B/B_{cr})\gamma_{c_i}^2 > 1$, where $B_{cr} = m_e^2 c^3 / (e\hbar)$. Here, $(B/B_{cr})\gamma_{c_i}^2$ is the peak energy of the synchrotron photons emitted by the i -th blob with temperature γ_{c_i} . Below $\nu \propto \gamma_{c,min}^2 B \gamma_{c,min}^2$ the Compton flux reveals the characteristic 1/3 slope, reflecting the low-energy synchrotron spectrum. In the Klein-Nishina regime, the exponential VHE cut-off mimics the shape of the electron cut-off, $F_\nu \propto \exp [-(\nu/\nu_{\max})^b]$, and is steeper compared to the synchrotron spectrum.

3. The origin of hard γ -ray flare spectra

Once a single component becomes dominant in the overall emission, as naturally expected for a flaring stage, hard spectral features can arise. This is more evident in the Compton part of the spectrum as (in the Thomson regime) the separation of the VHE peaks scales as $\sim \gamma_c^4$ and is greater than in the synchrotron case ($\sim \gamma_c^2$). The energetics of such a leading component, which is responsible for an observed flare, could change for different reasons: The total (intrinsic) energy offered to the accelerated particles or/and the temperature of the distribution could increase, for example, due to changes in the bulk flow properties or due to an increased injection of seed particles that undergo stochastic acceleration. Another possibility concerns an increase of the Doppler factor. Already a slight change of the line-of-sight angle to the observer during the propagation of a blob, could lead to the observation of a hard flare without an accompanying change of the intrinsic energetics of the components.

The aforementioned possibilities can be applied to explain the high-energy flare of Mkn 501 observed in 2009. To illustrate this, we assume for the "low state" that the total energy of each component drops as the temperature increases in order to account for a steeper than 1.5 spectrum. The scale assumed is $E \propto \gamma_c^{-1/4}$. For the flaring state the normalization of the two components with the highest temperatures is increased by a factor

of ~ 2 . Their temperature is also slightly increased. This leads to a hard high-energy flare above 10 GeV. Below 10 GeV the emission stays almost constant. Other parameters are kept the same for all blobs (i.e., magnetic field $B = 0.1$ G, blob radius $R = 10^{14}$ cm and Doppler factor $\delta = 30$). For this set of parameters, the synchrotron flux is lower than the one observed, implying that X-ray emission would have to come from a different part of the jet. This is consistent with the fact that little flux variation has been observed in X-rays.

4. Conclusion

Narrow energetic electron distributions, like relativistic Maxwellian-type ones, can successfully explain the very hard intrinsic γ -ray spectra that arise in some sources once EBL absorption is taken into account (Lefa et al. 2011).

Here we have demonstrated that the superposition of emission from such distributions could also accommodate more softer and broader γ -ray spectra. To show this, a multi-zone scenario was considered in which particles are accelerated through a stochastic acceleration process balanced by radiative (synchrotron/Thomson) losses in multiple zones characterized by different temperatures (i.e., achievable maximum electron energies). For the parameters examined here, particle escape can be neglected, and the particle distribution in each zone essentially takes a Maxwellian-type shape. Under reasonable conditions, the resultant overall (combined) particle energy spectra then approaches a power-law particle distribution $dN_e/d\gamma \propto \gamma^{-s}$ over the energy range corresponding to the lowest and the highest temperature, with power index s only depending on how the total energy (in non-thermal particles) in each component scales with temperature (cut-off Lorentz factor γ_c). In the case where all parameters, apart from the temperature, are kept constant (in particular the total energy in each component), the resultant power index approximates $s \rightarrow 2$. For similar magnetic fields and Doppler factors, softer/harder γ -ray spectra could arise when

the lower/higher temperature components dominate.

In this scheme, the dominance of one (or a few) of the radiating components could lead to a flaring state during which hard spectral feature become apparent. This leading component might increase its luminosity for different reasons, e.g., due to a change of the Doppler factor or the injected energy. As shown above, such a scenario can account for the 2009 flare in Mkn 501 during which a strong hardening of the emission spectra above 100 GeV has been observed (Abdo et al. 2011; Neronov et al. 2011). Mkn 501 is indeed known to be a source where detailed temporal and spectral modeling has provided evidence for the contributions of different components (such as a steady X-ray component plus a variable SSC component, see Krawczynski et al. 2002).

While in the present work an SSC approach has been employed, similar features are to be expected in external Compton scenarios. In the latter case, an even stronger spectral hardening up to $F_\nu \propto \nu$ may occur, while in the SSC case this is limited to $F_\nu \propto \nu^{1/3}$ (Lefa et al. 2011).

In summary, the "leading blob" model introduced here can explain in a natural way both the quiescent and flaring state in Mkn 501. It will be interesting to check to what extent this also applies to other sources.

REFERENCES

- Abdo, A.A. et al. 2011, *ApJ*, 727, 129
- Aharonian, F.A., Atoyan, A. M., & Nahapetian, A. 1986, *A&A*, 162, L1
- Aharonian, F.A. 2000, *NewA*, 5, 377
- Aharonian, F., et al. 2006, *Nature*, 440, 1081
- Aharonian, F., et al. 2007, *A&A*, 475, L9
- Derishev, E.V., Aharonian, F.A., Kocharovsky, V.V., Kocharovsky, Vl. V. 2003, *Phys. Rev. D*, 68, 043003
- Fritz, K.D. 1989, *A&A*, 214, 14
- Katarzyński, K., Ghisellini, G., Tavecchio, F., Gracia, J., & Maraschi, L. 2006, *MNRAS*, 368, L52
- Krawczynski, H., Coppi, C.S., & Aharonian, F. 2002, *MNRAS*, 336, 721
- Lefa, E., Rieger, F.M., & Aharonian, F.A. 2011, *ApJ*, in press (doi:10.1088/0004-637X/737/1/1)
- Lenain, J.-P., Boisson, C., Sol, H. & Katarzyński, K., 2008, *A&A* 478, 111
- Neronov, A., Semikoz, D. & A.M. Taylor 2011, *A&A* submitted (arXiv:1104.2801)
- Primack, J. R. et al. 2011, *Proc. of the 25th Texas Symposium* (eds. F.A. Aharonian, W. Hofmann, F.M. Rieger), *AIP Conf. Proc.* 1381, in press (arXiv:1107.2566)
- Schlickeiser, R. 1985, *A&A*, 143, 431
- Stawarz, L., & Petrosian, V. 2008, *ApJ* 681, 1725

Tavecchio, F., Ghisellini, G., Ghirlanda, G., Costamante, L., & Franceschini, A. 2009, MNRAS, 399, L59

Zirakashvili, V.N., & Aharonian, F. 2007, A&A, 465, 695

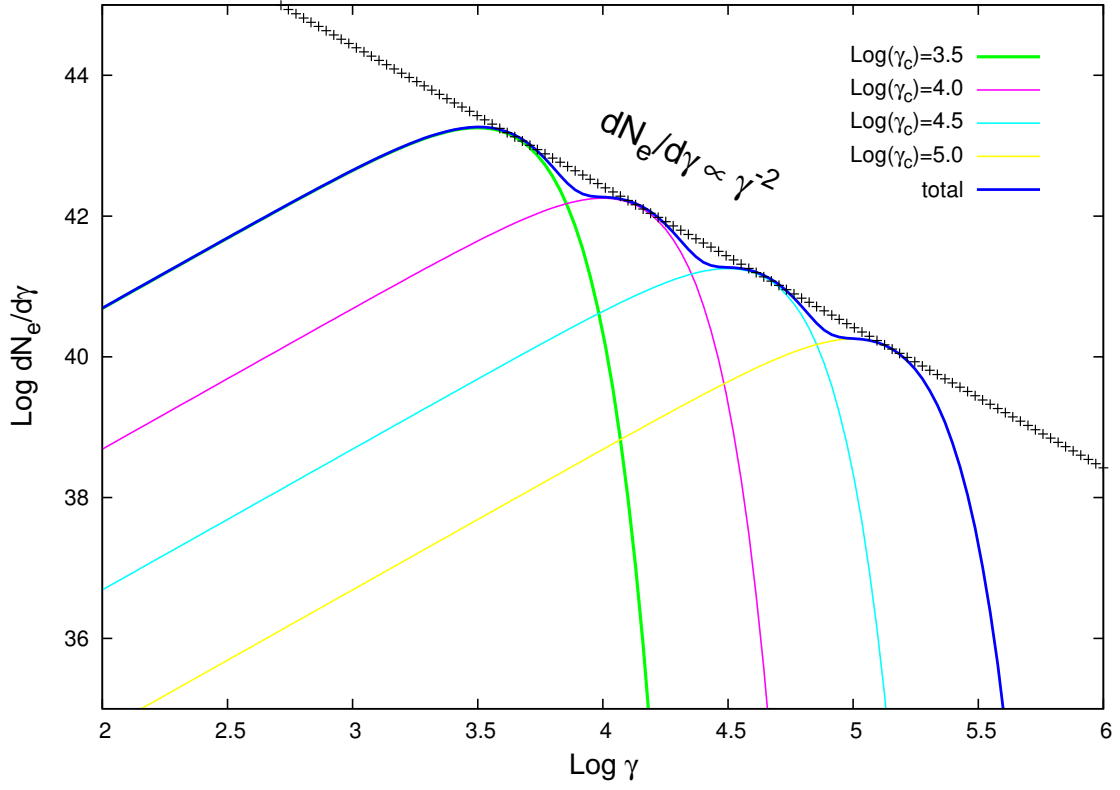


Fig. 1.— The total electron energy distribution from $N = 4$ blobs with different temperatures (γ_c) but the same total energy E_i tends to establish a power-law $dN_e/d\gamma \propto \gamma^{-2}$ between the minimum and maximum characteristic energies γ_c . Below $\gamma_{c,\min}$, $dN_e/d\gamma \propto \gamma^2$, whereas for $\gamma > \gamma_{c,\max}$ one has $dN_e/d\gamma \propto e^{-(\gamma/\gamma_{c,\max})^2}$. Here, the exponential cut-off index is $b = 2$ and other parameters used are $B = 0.1$ G and $E_i = 2 \times 10^{44}$ erg.

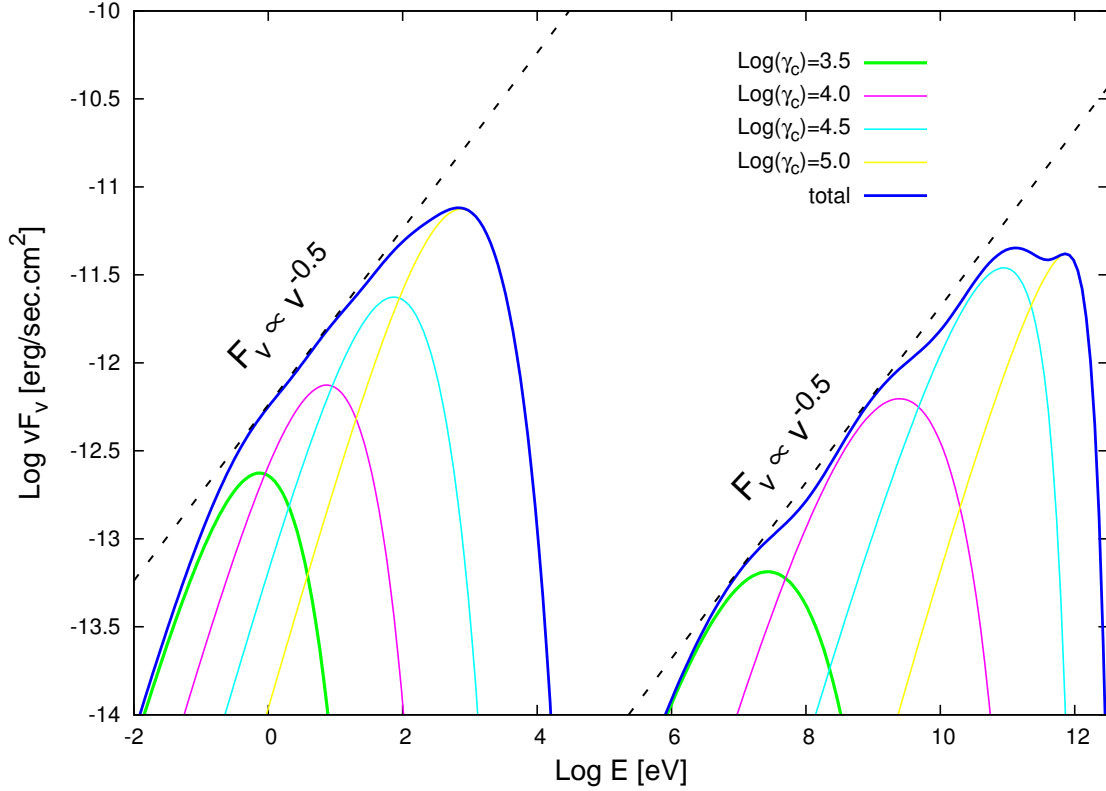


Fig. 2.— Resultant SSC emission from the combination of different components with Maxwellian-like electron distributions. The synchrotron flux exhibits a power-law behavior, $F_\nu \propto \nu^{-1/2}$, approximately between the energies related to the minimum and maximum temperature. The same holds for the Compton flux in the Thomson regime, while in the Klein-Nishina regime the spectrum becomes steeper. Doppler factor $\delta = 30$ and cut-off index $b = 2$ have been used. Other parameters are $R = 3 \times 10^{14}$ cm, $B = 0.1$ G, $E_i = 2 \times 10^{44}$ erg.

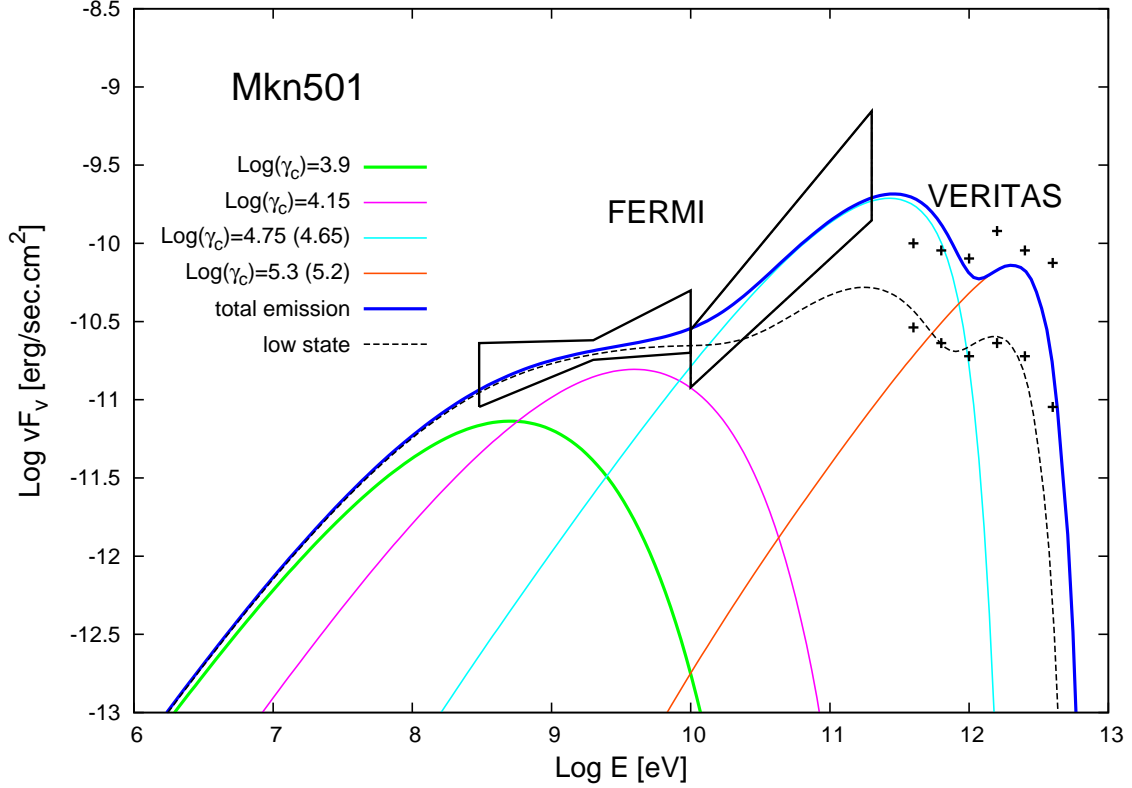


Fig. 3.— Resultant SSC emission from the sum of different ($N = 4$) blobs for the "low" (dashed-line) and "flaring state" (blue line) of Mkn 501. The total energy given to the particles scales as $E_i \propto \gamma_{ci}^{-1/4}$ and for the low state the temperatures are $\log(\gamma_c) = 3.9, 4.14, 4.6$ and 5.2 , respectively. Parameters kept constant are magnetic field $B = 0.1$ G, blob radius $R = 10^{14}$ cm, cut-off index $b = 3$ and Doppler factor $\delta = 30$. For the flaring state, the two blobs with highest temperatures are assumed to be enhanced by a factor of ~ 2 with their temperatures slightly increased (to 4.74 and 5.3 , respectively). Below 10 GeV, the flux is almost constant with respect to the low state. For data points, see Abdo et al. 2011 and Neronov et al. 2011.

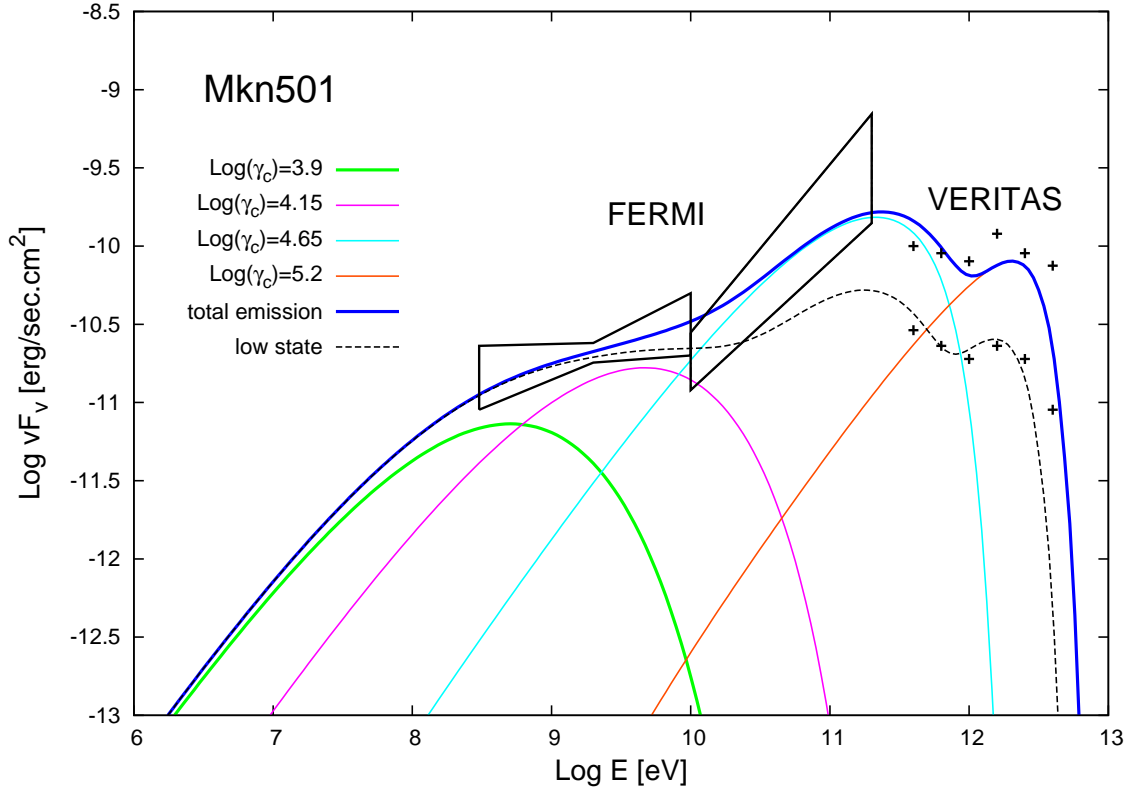


Fig. 4.— Same as figure 3 but assuming the flaring state to occur due to a change of the Doppler factor of the two components with the highest temperatures from $\delta = 30$ to $\delta = 40$.

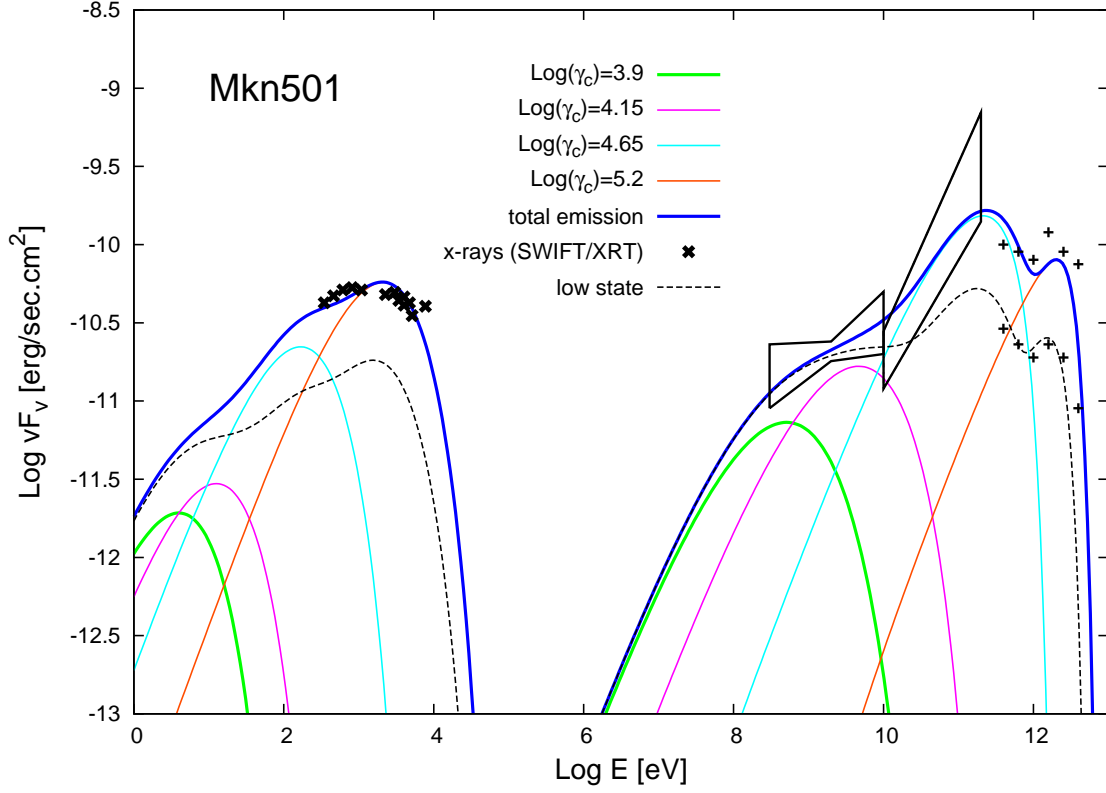


Fig. 5.— Same as figure 4 with the synchrotron part of the spectrum included. The X-ray regime is considered to be dominated by emission from a different part of the jet. Thus, during the flare no/little variability at X-ray energies would be observed as long as the synchrotron contribution from the "flaring" components does not exceed the measured X-ray data.